

Article

Combined Targeting of Estrogen Receptor Alpha and XPO1 Prevent Akt Activation, Remodel Metabolic Pathways and Induce Autophagy to Overcome Tamoxifen Resistance

Eylem Kulkoyluoglu-Cotul ¹, Brandi Patrice Smith ^{1,2} , Kinga Wrobel ¹, Yiru Chen Zhao ¹, Karen Lee Ann Chen ³, Kadriye Hieronymi ¹, Ozan Berk Imir ⁴, Kevin Duong ⁴, Caitlin O'Callaghan ^{5,6}, Aditi Mehta ^{5,6}, Sunati Sahoo ⁷, Barbara Haley ⁷, Hua Chang ⁸, Yosef Landesman ⁸ and Zeynep Madak-Erdogan ^{1,3,5,6,9,10,*} 

¹ Department of Food Science and Human Nutrition, University of Illinois, Urbana-Champaign, Urbana, IL 61801, USA; kulkoyl2@illinois.edu (E.K.-C.); brandis2@illinois.edu (B.P.S.);

kinga.wrobel@hotmail.com (K.W.); yiruster@gmail.com (Y.C.Z.); kadriye@hieronymi.de (K.H.)

² Illinois Informatics Institute, University of Illinois, Urbana-Champaign, Champaign, IL 61820, USA

³ Division of Nutritional Sciences, University of Illinois, Urbana-Champaign, Urbana, IL 61801, USA; kchen9282@gmail.com

⁴ School of Molecular and Cellular Biology, University of Illinois, Urbana-Champaign, Urbana, IL 61801, USA; berk.imir@gmail.com (O.B.I.); kduong6@illinois.edu (K.D.)

⁵ Cancer Center at Illinois, University of Illinois, Urbana-Champaign, Urbana, IL 61801, USA;

caitlinocallaghan22@gmail.com (C.O.); aditirmehta00@gmail.com (A.M.)

⁶ Beckman Institute for Advanced Science and Technology, University of Illinois at Urbana-Champaign, Urbana, IL 61801, USA

⁷ UTSW Medical Center, Dallas, TX 75390, USA; sunati.sahoo@utsouthwestern.edu (S.S.);

barbara.haley@utsouthwestern.edu (B.H.)

⁸ Karyopharm Therapeutics, Newton, MA 02459, USA; hchang@karyopharm.com (H.C.);

ylandesman@karyopharm.com (Y.L.)

⁹ National Center for Supercomputing Applications, University of Illinois, Urbana-Champaign, Urbana, IL 61801, USA

¹⁰ Carl R. Woese Institute for Genomic Biology, University of Illinois, Urbana-Champaign, Urbana, IL 61801, USA

* Correspondence: zmadake2@illinois.edu

Received: 27 February 2019; Accepted: 29 March 2019; Published: 4 April 2019



Abstract: A majority of breast cancer specific deaths in women with ER α (+) tumors occur due to metastases that are resistant to endocrine therapy. There is a critical need for novel therapeutic approaches to resensitize recurrent ER α (+) tumors to endocrine therapies. The objective of this study was to elucidate mechanisms of improved effectiveness of combined targeting of ER α and the nuclear transport protein XPO1 in overcoming endocrine resistance. Selinexor (SEL), an XPO1 antagonist, has been evaluated in multiple late stage clinical trials in patients with relapsed and/or refractory hematological and solid tumor malignancies. Our transcriptomics analysis showed that 4-Hydroxytamoxifen (4-OHT), SEL alone or their combination induced differential Akt signaling- and metabolism-associated gene expression profiles. Western blot analysis in endocrine resistant cell lines and xenograft models validated differential Akt phosphorylation. Using the Seahorse metabolic profiler, we showed that ER α -XPO1 targeting changed the metabolic phenotype of TAM-resistant breast cancer cells from an energetic to a quiescent profile. This finding demonstrated that combined targeting of XPO1 and ER α rewired the metabolic pathways and shut down both glycolytic and mitochondrial pathways that would eventually lead to autophagy. Remodeling metabolic pathways to regenerate new vulnerabilities in endocrine resistant breast tumors is novel, and given the need for

better strategies to improve therapy response in relapsed ER α (+) tumors, our findings show great promise for uncovering the role that ER α -XPO1 crosstalk plays in reducing cancer recurrences.

Keywords: breast cancer; endocrine resistance; nuclear transport pathways; XPO1; ER α ; metabolic rewiring

1. Introduction

The nuclear hormone receptor estrogen receptor alpha (ER α) is present in approximately 70% of both early and late stage human breast cancers [1,2]. ER α is targeted by endocrine therapies that are well tolerated and provide long-term disease-free survival if patients have localized disease [1]. Unfortunately, 30% of patients with ER positive (ER (+)) disease experience recurrence and metastasis, and there is a consistent long-term risk of death due to recurrent breast cancer with an even greater risk after 7 years [3–7]. Moreover, the 5-year relative survival of patients with ER (+) metastatic disease is 24%- almost none are cured and each year more women with recurrent ER (+) metastatic tumors die compared to women with ER (–) tumors [2,8].

Endocrine therapy is regarded as an effective treatment option for ER (+) metastatic cancer. Unfortunately, endocrine-resistance develops during the course of initial and subsequent endocrine treatment in almost all patients and occurs through various mechanisms including the mutational alterations in the ESR1 gene sequence, dysregulation in signaling pathways (i.e., Her2 signaling) and changes in drug uptake and metabolism [9]. Endocrine-resistant patients require increasingly toxic therapies. These are not optimal in terms of pharmacological properties due to poor tolerance and side effects that decrease the quality of the patient's life. Thus, endocrine resistance remains a significant clinical problem. A novel therapeutic approach to resensitize ER (+) metastatic tumors to endocrine therapies together with methods to select patients likely to benefit from this approach is needed. Without new strategies, many patients with ER (+) tumors will continue to face diminished prospects for long-term survival being prescribed regimens that decrease their quality of life without receiving clinical benefit.

Tamoxifen (TAM) remains the “first-in-line” endocrine therapy and is regarded as one of the most effective treatments for patients diagnosed with ER (+) breast cancer. While several recent trials showed that aromatase inhibitors (AIs) in combination with ovarian suppression were effective in premenopausal breast cancer treatment, the American Society for Clinical Oncology (ASCO) continues to recommend TAM for premenopausal women [5]. This may be attributed to the observation that AIs may also have significant adverse side effects in some postmenopausal women, such as increased joint pain, bone fractures, and risk of cardiovascular disease [1,5,10]. Therefore, TAM remains as an important endocrine therapeutic agent in both pre- and post-menopausal women and is expected to continue to be widely used for some time.

In our previously published study, which sought to understand the mechanism of TAM resistance in a preclinical setting, we identified a group of nuclear transport proteins, including exportin 1 (XPO1), which were upregulated in TAM-resistant cell lines and tumors [11]. Importantly, XPO1 upregulation caused nuclear export of ERK5, which is necessary in the nucleus for proper transcriptional response of ER α to TAM. Moreover, when ERK5 translocates to the cytoplasm, it can partner with other cytoplasmic proteins, including actin reorganization proteins that contribute to cancer cell motility. However, it is not known whether XPO1 activates other mechanisms that may be targeted by therapies in current use, specifically for endocrine therapy resistant and ER (+) breast cancers.

Based on previous studies, [11–13], we hypothesized that ER α and XPO1 work together to drive TAM-resistance, and that combined targeting would more effectively sustain tumor regression than targeting either protein alone. Specifically, we showed that XPO1 mRNA levels were higher in Luminal B subtype of tumors which are more refractory to endocrine treatments, and that high XPO1 expression values were associated with a poor outcome in all women who were treated with TAM [11]. Therefore,

XPO1 could be an excellent therapeutic target in breast cancer as XPO1 is already targeted in other therapy-resistant cancers with the highly specific small molecule inhibitor SEL, which is an orally active and well-tolerated drug [14,15]. Our rationale is that targeting XPO1 together with ER α is clinically relevant and combining TAM with SEL potentially offers higher efficacy, specificity, and lower toxicity for the treatment of endocrine resistant, recurrent ER (+) breast cancer.

To evaluate the effects of combining TAM (4-OHT) with SEL, in the present study we used transcriptome analysis and found that the combination differentially modulated Akt signaling-associated gene expression as well as glycolytic and mitochondrial gene expression programs. Because of differential changes in Akt phosphorylation with 4-OHT and/or SEL, we hypothesized that metabolic pathways associated with Akt activity and consequently the metabolic profile of breast cancer cells would change in the presence of 4-OHT and SEL. We demonstrated that combined targeting of XPO1 and ER α in TAM-resistant cell lines shuts down metabolic pathways that would eventually lead to autophagy. Our studies provide a novel mechanism of action of combined targeting of ER α and XPO1 to overcome TAM resistance in recurrent ER α (+) breast cancer.

2. Materials and Methods

2.1. Cell Culture and Ligand Treatments

All cell lines were obtained from American Type Culture Collection (Waltham, MA, USA). MCF-7 cells were cultured in Improved Minimal Essential Medium (MEM) with NEAA salts (Sigma, St Louis, MO, USA), supplemented with 10% fetal bovine serum (FBS) (HyClone, Logan, UT, USA), 100 μ g/mL penicillin/streptomycin (Invitrogen, Carlsbad, CA, USA) and 1500 mg/L sodium bicarbonate (Gibco, MA, USA). *Acquired resistance* was studied from resistance progression cell lines previously derived and characterized by long-term exposure of parental MCF-7 cells to 4-OH-Tam (MCF-7 Tam^R) [11,16]. These cells retain ER α expression, do not require E2 for growth, are not growth inhibited by SERMs and 4-OH-Tam stimulates their growth [11,16]. Human breast cancer cell lines BT474, HCC-1500 and MDA-MB-134, which are 4-OH-Tam-resistant, were used as a model of *de novo resistance* [11,17,18]. BT474 were cultured in ATCC recommended Hybri-care medium with 10% inactivated FBS, sodium bicarbonate and antibiotics. MDA-MB-134 cells were cultured in Leibovitz's medium with 20% FBS (HyClone), and 100 g/mL penicillin/streptomycin (Invitrogen). HCC-1500 cells were cultured in ATCC-formulated RPMI1640 media with 10% FBS, sodium bicarbonate and antibiotics. Before ligand treatments, cells were grown in the corresponding phenol red-free media at least for three days.

For isobologram analysis, BT474 and MCF-7 Tam^R cells were seeded at a density of 2×10^3 cells/well in a 96-well plate, and were grown overnight in IMEM media without phenol red. On day 1, cells were treated with different doses of 4-OHT (from 10^{-9} M to 10^{-5} M) (Sigma) and SEL (from 10^{-9} M to 10^{-5} M) (Selleckchem, Houston, TX, USA) alone and in combination. Treatment was repeated again on day 4. On day 7, WST1 assay (Roche Molecular Systems, Inc., Pleasanton, CA, USA) was used to quantify cell proliferation ratio. Absorbance was measured at 450 nm using a Cytation5 plate reader (BioTek, Winooski, VT, USA). IC₅₀ and isobologram calculations were made based on literature (*) by using Microsoft[®] Office Excel (Seattle, WA, USA) and statistical analyses were done by using Graphpad[®] Prism8 software (GraphPad Software Inc., La Jolla, CA, USA, www.graphpad.com). All experiment conditions had six technical repeats and experiments were repeated at least for three times.

2.2. RNA Sequencing Analysis

RNASeq analysis was performed as previously described [19–21]. Briefly, BT474 cells were treated with Vehicle (Veh, 0.5% EtOH), 10^{-6} M 4-OHT (Sigma), 10^{-7} M Selinexor (SEL) (Selleckchem) or 4-OHT+SEL combination for 24 h. Concentrations of ligands are based on our previously published study [11] and clinical data [22–24]. Total RNA was extracted with TRIzol reagent (Life Technologies, Carlsbad, CA, USA) according to the manufacturer's protocol and cleaned using a clean-up kit

(QIAGEN, Hilden, Germany). RNA quality was assessed using bioanalyzer. Total RNA from each sample (three per treatment group) were sequenced at the UIUC sequencing center, and data was generated in Fastq file format to compare the expressions between the four treatment groups.

Preprocessing and Quality Control: Fastq files containing raw RNA sequencing data were trimmed using Trimmomatic (Version 0.36) [25]. Next, the reads were mapped to the *Homo sapiens* reference genome (GRCh37) from the Ensembl [26] database and aligned using the STAR alignment tool (Version 2.5.3) [27]. After this, the read counts were generated from SUBREAD (Version 1.5.2) [28] and featured counts were exported for statistical analysis in R. Quality control and normalization was conducted in R using edgeR (Version 3.20.9) [29].

Statistical Analysis and DEGs: Statistical analysis was conducted in R using limma (Version 3.34.9) [30,31]. Empirical Bayesian statistics were conducted on the fitted model of the contrast matrix. Differentially expressed genes were then determined by fold-change and *p*-value with Benjamini and Hochberg [32] multiple test correction for each gene, for each treatment relative to the vehicle control. We considered genes with fold-change >1.5 and *p*-value < 0.05 as statistically significant, differentially expressed. Cluster3 software was used for clustering the differentially expressed genes. Data was visualized using Treeview Java. PCA analysis was performed using StrandNGS (Version 3.1.1). GSEA [33,34] analysis was used to identify GO terms associated with different treatments.

2.3. *In Vivo* Xenograft Study, Immunohistochemistry Staining (IHC) and Data Analysis

All experiments involving animals were conducted with protocols approved by the University of Illinois at Urbana-Champaign and by the National Institutes of Health standards for use and care of animals (IACUC Protocol 14193). Tumor xenograft studies were performed using the BT474 cell line in immunocompromised female mice as previously described [11,35,36]. Briefly, 6-week-old BALB/c athymic, ovariectomized, nude female mice from Taconic Biosciences (Germantown, NY, USA) were used. After one week of acclimatization, 0.72 mg, 60-day release E2 pellets from Innovative Research of America (Sarasota, FL, USA) were implanted subcutaneously to maintain a uniform level of estrogen. The next day 2.5×10^7 BT474 cells resuspended in 50% PBS and 50% Matrigel were injected subcutaneously into both right and left flank of each mouse. Once the tumor size reached 200 mm³, five animals were randomized to each treatment group. Half of the mice were implanted with vehicle pellets and the other half were implanted with 25 mg, 60-day release TAM pellets from Innovative Research of America. Each group was randomized to Vehicle or SEL injection (20 mg/kg). Concentration was selected based on clinically relevant dose [22–24]. Biweekly injections were performed (Monday and Friday) for 4 weeks. Each mouse was housed individually. Animals were monitored daily by the veterinarians for any signs of starvation, dehydration, stress, and pain. Total weight, food intake, and tumor size was monitored using a digital caliper biweekly. Tumors were removed from euthanized mice at the end of the experiment or at the time when tumor size reached 1000 mm³ and were fixed in 10% neutral-buffered formalin, processed, and embedded in paraffin in 2 M sucrose before being frozen in cutting medium. Tissues were cut in 5 microns by using a microtome (RM1255, Leica, Wetzlar, Germany). For both pAkt S473 and pAkt T308 immunostainings, tissues were deparaffinized and hydrated through graded alcohols to water. Antigen retrieval was performed by using citrate buffer, pH 6.0 in a streamer for 1 h. Samples were blocked in hydrogen peroxide for 10 min. To remove non-specific protein staining, samples were blocked with Background buster (Innovex Biosciences, Richmond, CA, USA) for 10 min and rinsed with TBS-Tween solution, pH 7.6. Then, samples were incubated with pAkt S473 primary antibody (#4060, Cell Signaling, Danvers, MA, USA) overnight at 4 °C and with pAkt T308 primary antibody (#13038, Cell Signaling) for 1 h at room temperature at 1:100 dilution. After rinsing with TBS-Tween solution, pH 7.6., samples were stained with secondary anti-rabbit and anti-mouse HRP-Polymer (Biocare Medical, Concord, CA, USA) for 30 min. Finally, samples were incubated with DAB (Innovex, Richmond, CA, USA) for 5 min and counterstained with hematoxylin, dehydrated and mounted on slides. Results are from at least four tumors per treatment. Visualization of the samples were performed with Nanozoomer Slide Scanner

(Hamamatsu, Japan) at 80× magnification and positive staining quantification was performed by NDP.view software (Ver. 2.7.39, Hamamatsu Photonics, Ichinocho, Japan). Five fields per tumor were imaged and quantified. Representative images are presented.

For the verification of XPO-1 protein levels in patient tumor samples, BRC1021 tissue microarray from Pantomics, Inc. (Richmond, CA, USA) containing 95 cases with known ER, PR, AR, Her2, p53, EGFR, and Ki67 IHC results was used. Subtype of tumors were based on following criteria: Lum A: ER (+), Her2 (−), Ki67 < 15; Lum B: ER (+), Her2 (+) or ER (+), Her2 (−), Ki67 > 15; Her2 (+): ER (−), Her2 (+); TNBC: ER (−), PR (−), Her2 (−) [37,38]. XPO1 antibody was from Bethyl laboratories (A300-469A). BRC1021 TMA included 43 Her2, 3 LumA, 31 Lum B, 17 TNBC tumor samples. UTSW cohort included 50 Luminal A, 45 Luminal B, 48 TNBC and 35 Her2 positive/amplified breast tumors validated by a pathologist. The samples were collected under the STU 102010-051 IRB protocol number, were collected at UTSW, and affiliated hospitals. For each core, a score for XPO1 was assigned based on the signal intensity (0 = none, 1 = low, 2 = moderate, and 3 = high).

2.4. Western Blot Analysis in Cell Lines

Cells were seeded on 30 mm cell culture plates at 1×10^5 cells/well concentration in corresponding treatment media without phenol red which contains 5% FBS. Cells were treated with 4-OHT (10^{-6} M) (Sigma) and SEL (10^{-7} M) (Selleckchem)-containing treatment media overnight. Next day, cells were collected in Lysis buffer (0.5 M EDTA, 1 M TrisHCl pH 8.1, 10% SDS, 10% Empigen, ddH₂O) with 1× Complete Protease Inhibitor (Roche) and 1× Phosphatase Inhibitor (Thermo Scientific, Waltham, MA, USA). Samples were further processed with sonication and protein concentrations were determined by BCA assay (Thermo Scientific). Then, samples were boiled in SDS-containing loading buffer and were run in 10% precast gels (BioRad) and transferred to nitrocellulose membrane. The membrane was blocked in Blocking Buffer (Odyssey[®], Li-Cor, Lincoln, NE, USA) and target proteins were probed with XPO1 (sc-74454, Santa Cruz Biotechnology, Dallas, TX, USA), p-Akt S473 (#4060, Cell Signaling), pAkt T308 (#13038, Cell Signaling), Akt (#9272, Cell Signaling), PARP (#9542, Cell Signaling), ATG9A (STJ98598, St. John's Laboratory, London, UK), AMBRA-1 (STJ98593, St. John's Laboratory) and Beclin-1 (STJ 98594, St. John's Laboratory), antibodies in 1:1000 dilution and β-actin (Sigma SAB1305546) antibody in 1:10000 dilution. The secondary antibodies were obtained from Odyssey were used at 1:10000 dilution. The membranes were visualized by using Licor Odyssey CLx infrared imaging device and software. All results were repeated at least three times and the results were normalized according to signal, which was received from β-actin loading control. Representative blots are presented.

2.5. Seahorse Metabolic Profiling Assays

MCF-7, MCF-7 Tam^R and BT474 cells were seeded at a density of 5×10^4 and MDA-MB-134 and HCC 1500 cells were seeded at a density of 1×10^5 in corresponding treatment media without phenol red in each well of the XFp Cell Culture miniplates, respectively (Seahorse Bioscience Inc., Billerica, MA, USA). The FCCP concentration was 0.5 μM for MCF-7, BT474, MDA-MB-134 and HCC 1500 cells. Next day, cells were treated with 4-OHT (10^{-6} M) (Sigma) and/or SEL (10^{-7} M) (Selleckchem)-containing treatment media overnight and the cartridges were hydrated with the calibration solution and kept in a non-CO₂ incubator at 37 °C overnight. In parallel, a duplicate of each plate was used for cell counting to monitor cell number changes after 24 h of treatments and Seahorse data was normalized to total cell number. On the assay day, cells were washed with XF Base Media without phenol red (Seahorse Bioscience Inc.) supplemented with 10 mM L-glucose, 2 mM L-glutamine (Gibco) and 1 mM sodium pyruvate (Gibco, Waltham, MA, USA). The ECAR (mpH/min) and OCR (pmol/min) values were obtained by using Seahorse XFp Cell Energy Phenotype Test Kit (Seahorse Bioscience Inc.), Seahorse XFp Mito Stress Test Kit (Seahorse Bioscience Inc.), Seahorse XFp Glycolytic Stress Kit (Seahorse Bioscience Inc.), and Seahorse XFp Mito Fuel Flex Test Kit (Seahorse Bioscience Inc.), which were run with Seahorse XFp Analyzer (Seahorse Bioscience Inc.). Experiments were performed in triplicate and repeated at least three times.

2.6. Caspase Colorimetric Protease Assay

MCF-7 and BT474 cells were seeded at a density of 2×10^3 cells to a 96-well plate and in the next day, they were treated with 4-OHT (10^{-6} M) (Sigma) and SEL (10^{-7} M) (Selleckchem) alone and in combination for 24 h. The colorimetric caspase activities of Caspase 2, Caspase 3, Caspase 6, Caspase 8 and Caspase 9 were determined according to the manufacturer recommendations by using ApoTarget Caspase Colorimetric Protease Assay Sampler Kit (Invitrogen, Carlsbad, CA, USA). Changes in colorimetric density were detected by Cytation™ 5 Cell Imaging Multi-Mode Plate Reader (Biotek Instruments, Inc., Winooski, VT, USA) at 400 nm wavelength. Experiments were performed in duplicates and repeated three times.

2.7. Autophagy Assay

MCF-7 and BT474 cells were seeded at a density of 2×10^3 cells to 96-well plate and in the next day, they were treated with 4-OHT (10^{-6} M) (Sigma) and SEL (10^{-7} M) (Selleckchem) alone and in combination for either 24 or 48 h. Autophagosome formation was detected through GFP-labelled LC3-II protein in live cells using the Cyto-ID Autophagy Detection Kit (Enzo Life Sciences, Farmingdale, NY, USA) according to manufacturer recommendations by Cytation™5 Cell Imaging Multi-Mode Plate Reader (Biotek Instruments Inc.) at ~480 nm excitation and ~530 nm emission. In addition, Hoechst 33342 Nuclear Stain was also recorded by means of DAPI filter set at ~340 nm excitation and ~480 nm emission. For flow cytometry analysis, BT474 cells were seeded at a density of 1×10^6 cells/plate, and they were grown for 48 h in IMEM media without phenol red. Next day, cells were treated with 4-OHT (10^{-6} M) (Sigma) and SEL (10^{-7} M) (Selleckchem) alone and in combination for 24 h. Negative control plates were treated with EtOH and positive control plates were also treated with Rapamycin (5×10^{-6} M) (CytoID) for 24 h. Following the treatment process, cells were collected and centrifuged at 1000 rpm for 5 min in $1 \times$ Assay buffer provided in the CytoID® Autophagy Detection Kit (Enzo Biosciences Inc, Ann Arbor, MI, USA). Cells were resuspended again and incubated with CYTO-ID® Green Detection Reagent for 30 min at dark. After this incubation time, cells were washed with $1 \times$ Assay buffer 3 times and results were analyzed with results were analyzed by BD™ LSR II Flow cytometry analyzer (BD Biosciences Inc., San Jose, CA, USA). Following analysis, results were analyzed by FCS Express 6 Flow Cytometry Software (DeNovo Software) (<https://www.denovosoftware.com/site/Flow-RUO-Overview.shtml>) and all experiments were repeated with three technical replicates at least three times. Experiments were performed in duplicates and repeated three times.

For the inhibition of autophagy experiments, BT474 cells were seeded in 96-well plates at a confluency of 2000 cells/well in corresponding treatment media. At day 2, they were treated in a media with 10^{-6} M 4-OHT and 10^{-7} M SEL alone or combined in the presence or absence of 10^{-5} Chloroquine (Sigma). This treatment was repeated at day 5. Cellular viability was measured with WST1 reagent (Roche) at 450 nm wavelength and results were quantified by using Cytation5 cell imaging Multi-Mode reader (Biotek Instruments Inc.). Statistical analyses were done by using GraphPad Prism8© software.

2.8. Cell Cycle Analysis

Flow cytometry analysis was performed as previously described [11,16,39]. Briefly, MCF-7 and BT474 cells were seeded at a density of 1×10^6 cells/plate and their media was changed two times in every two days. Following an overnight treatment with 4-OHT (10^{-6} M) (Sigma) and SEL (10^{-7} M) (Selleckchem) alone and in combination, cells were collected with 0.1% FBS containing $1 \times$ PBS, washed, resuspended at $1-2 \times 10^6$ cells/mL and fixed with ice cold ethanol for 24 h. Next day, cells were washed with $1 \times$ PBS and incubated in 10 ng

RNAase for one hour at room temperature. Cells were stained with 0.25% Propidium Iodide (#10008351, Cayman Chemicals, Ann Arbor, MI, USA) for one hour and results were analyzed

by BD™ LSR II Flow cytometry analyzer (BD Biosciences Inc., San Jose, CA, USA). Following analysis, results were analyzed by FCS Express 6 Flow Cytometry Software (DeNovo Software, <https://www.denovosoftware.com/site/Flow-RUO-Overview.shtml>) and all experiments were repeated three times.

2.9. Statistical Analyses

Data from all studies were analyzed using a one-way analysis of variance (ANOVA) model to compare different ligand effects, a two-way-ANOVA model to compare time-dependent changes. All data was tested for normal distribution using pairwise *t* tests with a Bonferroni correction. All data was normally distributed unless otherwise noted. Normally distributed data was analyzed using pairwise *t* tests with a Bonferroni correction to identify treatments that were significantly different from each other (* $p < 0.05$, ** $p < 0.01$, *** $p < 0.001$, **** $p < 0.0001$). For every main effect that was statistically significant at $\alpha = 0.05$, pairwise *t*-tests were conducted to determine which ligand treatment levels were significantly different from each other. For these *t*-tests, the Bonferroni correction was employed to control experiment wise type I error rate at $\alpha = 0.05$ followed by Bonferroni post hoc test. Data that were not normally distributed were analyzed using Mann Whitney test for nonparametric data (* $p < 0.05$, ** $p < 0.01$, *** $p < 0.001$, **** $p < 0.0001$). Statistical significance was calculated using GraphPad Prism for Windows.

2.10. Availability of Data and Materials

Gene expression data is submitted to GEO database under the accession number GSE112883 and going to be available from the day of the acceptance of the manuscript.

3. Results

3.1. 4-OHT+SEL Treatment Synergistically Sustains Tumor Regression in Endocrine Resistant Luminal B Subtype Breast Cancer Cells

Our previous study showed that XPO1 mRNA was overexpressed in the Luminal B subtype of tumors, which are more likely to recur on endocrine treatments relative to the Luminal A subtype [11]. To validate our results, we performed IHC analysis for XPO1 protein expression in two independent breast tumor sets with samples from various breast cancer subtypes. This analysis showed that Luminal B subtype tumors have higher overall XPO1 signal intensity and percentage XPO1 positive cells in two independent cohorts of breast tumors (Figure 1A,B). We then treated endocrine resistant BT474 cells with 4-OHT, SEL or both in combination to assess whether these treatments synergized to reduce cell viability. The isobologram analysis showed that the 4-OHT and SEL combination synergized to achieve a greater decrease in cell viability than with either agent alone (Figure 1D). These results are consistent with our BT474 xenograft studies in nude mice, which showed that the tamoxifen (TAM) and SEL combination provided complete tumor regression, which was sustained several weeks after cessation of drug administration (Figure 1E) [11].

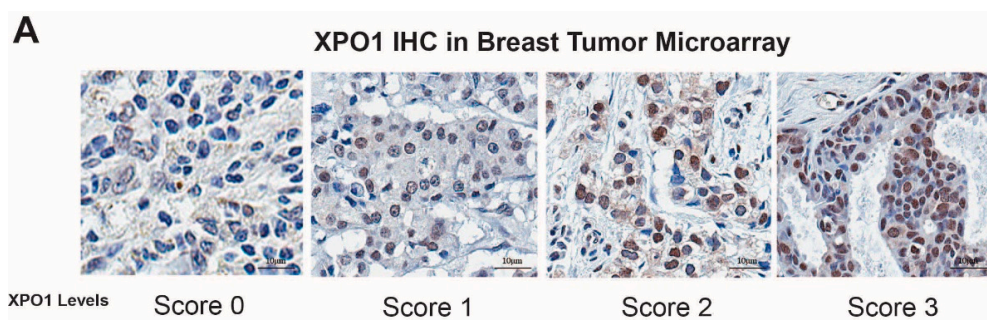


Figure 1. Cont.

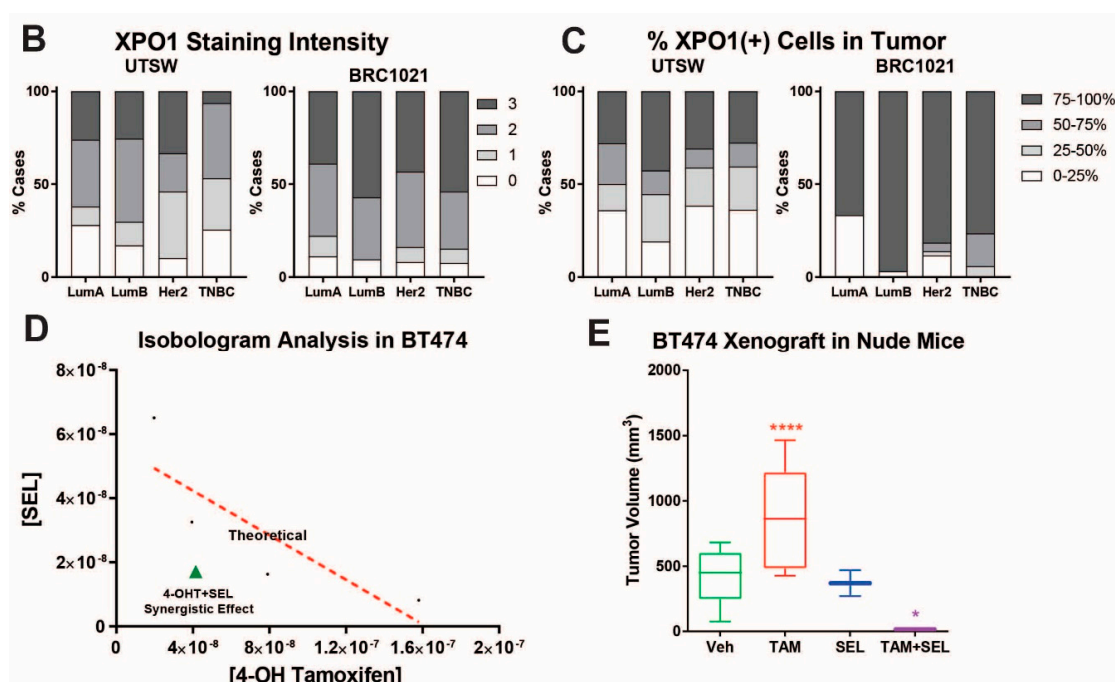


Figure 1. XPO1 is overexpressed in Luminal B breast cancers and targeting XPO1 modulates Akt signaling. (A) Verification of XPO-1 protein levels in patient tumor samples (BRC1021 from Pantomics, Inc containing 95 cases with known ER, PR, AR, Her2, p53, EGFR, and Ki67 IHC results). For each core, a score for XPO1 was assigned based on the signal intensity (0 = none, 1 = low, 2 = moderate, and 3 = high). (B) XPO1 staining intensity from (A). (C) Percentage of XPO1 positive cells from (A). (D) Isobologram analysis of synergy between 4-OHT and SEL in BT474 cells. (E) BT474 xenograft experiment showing that combined targeting of ER α and XPO1 provided sustained tumor regression. (Adapted from [11]). * $p < 0.05$, **** $p < 0.0001$

3.2. 4-OHT+SEL Combination Treatment Causes Gene Expression Changes Distinct from 4-OHT and SEL Treatments Alone in TAM-Resistant Cell Lines

To understand how the TAM+SEL combination provide a sustained tumor regression, we performed a global gene expression analysis in BT474 cells that were treated with Veh, 4-OHT, SEL or 4-OHT+SEL. Hierarchical clustering of the differentially-expressed genes revealed 10 clusters with different gene regulation patterns. Genes in Clusters 1, 2, 3, 6, 9 and 10 were regulated similarly with all treatments. The 4-OHT+SEL combination and 4-OHT alone resulted in similar patterns of regulation for genes in Cluster 1. The 4-OHT+SEL combination and SEL alone caused similar gene regulation patterns for genes in Clusters 2, 3, 6, 9 and 10. On the other hand, Clusters 4 and 5 include genes that were upregulated more with the combination treatment than either treatment alone, and genes in Clusters 7 and 8 were downregulated more with the combination treatment than either treatment alone (Figure 2A,B). Principle component analysis (PCA) showed that treatment groups differed significantly (Figure 2C). Venn-diagram analysis of up- and down-regulated genes revealed that the combination treatment caused gene expression changes similar to as well as different from single agent treatments. The combination treatment increased the expression of 101 genes and decreased the expression of 132 genes that were not affected by either treatment alone (Figure 2D,E).

Next, we used Gene Set Enrichment Analysis (GSEA) analysis to identify functional gene groups that were associated with different treatments (Supplementary Figure S1). The 4-OHT treatment caused upregulation in genes for cell cycle-, endocrine therapy resistance-, and breast cancer invasiveness-related pathways. On the other hand, genes involved in apoptosis and decreased tumor invasiveness were downregulated by this treatment.

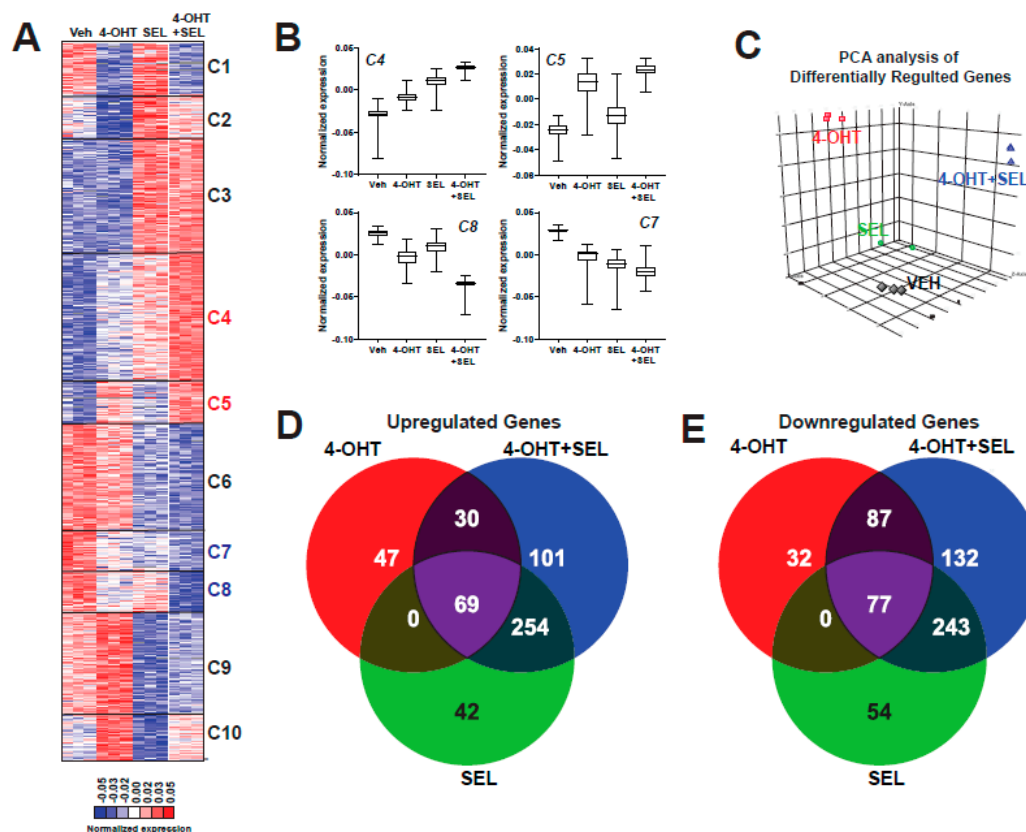


Figure 2. The 4-OHT+SEL combination treatment causes gene expression changes distinct from 4-OHT or SEL treatments alone in TAM resistant cell lines. (A) Hierarchical clustering of differentially expressed genes. (B) Average expression profiles of clusters that showed differential regulation by the 4-OHT+SEL combination. (C) PCA analysis Venn diagram analysis of Upregulated (D) and Downregulated (E) genes by different ligands.

Although SEL was effective in decreasing endocrine therapy resistance, breast cancer invasiveness, and metastasis related genes, genes that would regulate apoptosis were also downregulated by this treatment. The 4-OHT+SEL combination was the most effective treatment for down regulating therapy resistance and tumor invasiveness. Specifically, the combination treatment was more efficient than either treatment alone to upregulate gene sets associated with genes downregulated in Luminal B tumors, metastasis, and in bone metastasis. However, the combination treatment was very effective in downregulating ER α target genes that were upregulated by AKT1 overexpression and genes that were upregulated in Luminal B tumors, endocrine therapy resistance and metastasis that were identified in various studies. These findings are consistent with our data showing that differential Akt signaling was modulated by the ER α and XPO1 crosstalk. Of note, 4-OHT+SEL reduced targets of FGFR1 signaling, recently shown to be associated with Palbociclib + Fulvestrant-resistant tumors [40,41]. Overall, our gene expression analysis showed that the 4-OHT+SEL treatment was very effective in downregulating genes associated with endocrine resistance and metastasis. Data on other gene sets associated with metabolic regulation and autophagy will be presented in the upcoming sections.

3.3. XPO1 Inhibition Modulates Differential Akt Phosphorylation in TAM-Resistant Cells and Tumor Xenografts

We next focused on the Akt signaling associated gene sets which were identified as differentially downregulated by the 4-OHT+SEL combination (Figure 3A) because they play an important role in cell survival and metabolism. We validated differential Akt phosphorylation with individual or combined drug treatments in BT474 cells (Figure 3B) and MCF-7 TAM^R cells (Supplementary Figure

S2). Of note, 4-OHT treatment induced an increase in the cytoplasmic pAkt Ser473 signal, whereas SEL treatment increased the pAkt Thr305 signal in dividing cells (arrows) (Figure 3C). As we previously showed, TAM treatment stimulated tumor growth in BT474 tumor xenografts, whereas SEL treatment inhibited tumor growth [11]. However, tumor growth resumed within 3 weeks after SEL treatment was stopped. By contrast, the combination of SEL and TAM not only caused a faster and more complete regression of tumors, but the regression was also sustained [11]. To validate our pathway analysis in vivo, we utilized tumor xenograft samples from this experiment (Figure 3D).

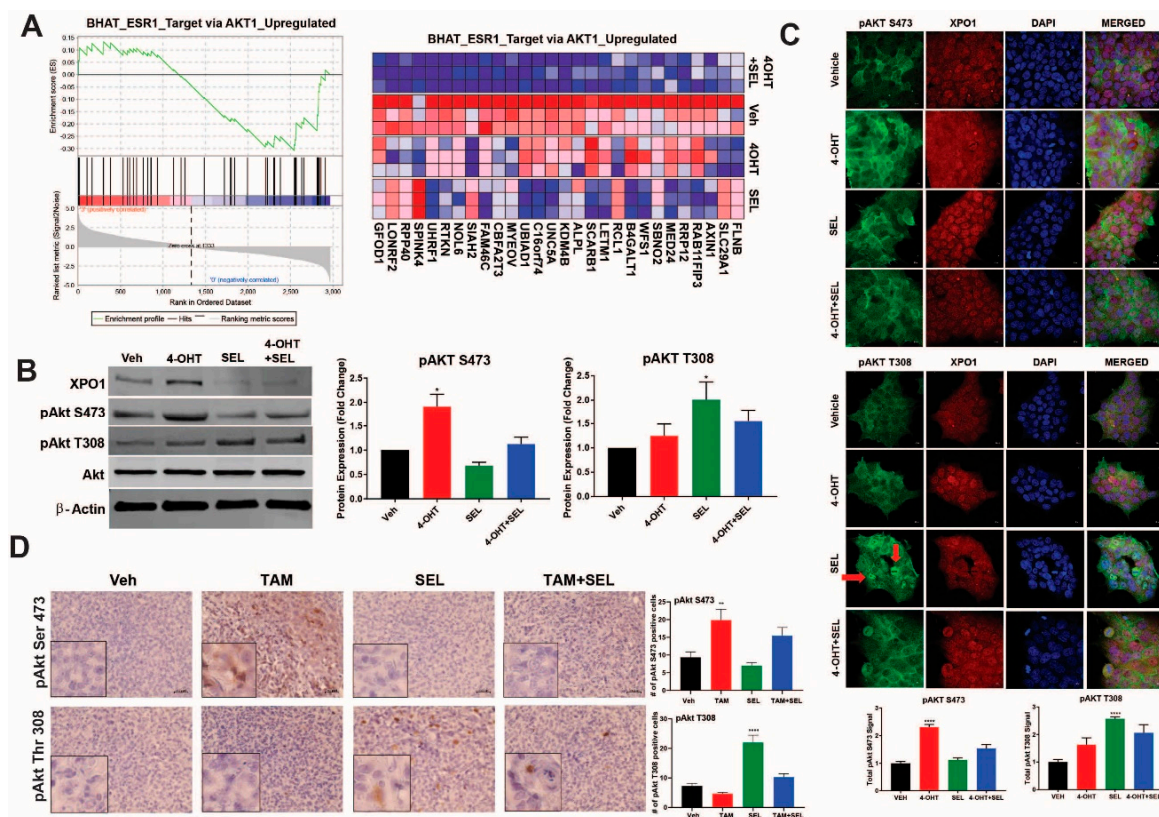


Figure 3. XPO1 inhibition modulates differential Akt phosphorylation in TAM-resistant cells and tumor xenografts. (A) GSEA analysis of RNA-Seq data depicting regulation of Akt signaling by the 4-OHT+SEL combination. ER α -XPO1 targeting changed XPO1 and pAkt protein expressions in both TAM-sensitive and TAM-resistant breast cancer cell lines. Western blot analysis (B) and immunofluorescence analysis ($* p < 0.05$) (C) of BT474 cells treated with 4-OHT (10^{-6} M) and SEL (10^{-7} M) for 24 h alone and in combination. Protein expression was quantified and is shown in bar graphs. A one-way analysis of variance (ANOVA) model was used for statistical significance of treatment effect and values were presented as mean \pm SEM from three independent experiments ($* p < 0.05$, $** p < 0.01$). scale bar = 200 pixels. (D) IHC staining of pAkt T308 and pAkt S473 in tumor samples obtained from BT474 xenografts received individual and combined TAM and SEL treatments (from Figure 1C). In the figure, red-brownish staining represents pAkt T308 and pAkt S473 proteins. This figure showed that individual 4-OHT and SEL treatments activated two different phosphorylation sites of Akt protein. The top panel indicated that SEL treatment activated pAkt T308 phosphorylation in BT474 tumor xenografts. The bottom panel showed that TAM treatment activated pAkt S473 phosphorylation in BT474 tumor xenografts. Quantification of positive staining was performed digitally by selecting four independent regions on the sample slides and the results were given in the corresponding graphs. Statistical significance was presented as mean \pm SEM by using one-way analysis of variance (ANOVA) model ($** p < 0.01$, $**** p < 0.0001$). scale bar = 20 μ m.

Our IHC analysis showed that Ser 473 phosphorylation of Akt protein increased only in tumors from TAM treated animals, whereas Thr 308 phosphorylation of Akt was more prevalent in tumors from SEL treated animals. Both of the phosphorylation events were dampened in tumors from animals that were treated with the SEL+TAM combination, suggesting that the combination treatment prevented activation of survival pathways that were otherwise prominent when tumors were treated with single agents (Figure 3D). These results suggest that ER α -XPO1 crosstalk might contribute to drug resistance by regulating differential Akt signaling, which is important for survival and metabolic control.

3.4. ER α -XPO1 Targeting Changes the Metabolic Phenotype of Breast Cancer Cells from An Energetic to A Quiescent Profile

Our gene expression analysis also pinpointed two of the pathways associated with metabolic regulation: glycolysis and mitochondrial respiration (Figure 4A,B). Since Akt is a major regulator of cell metabolism and TAM responsiveness, we hypothesized that XPO1 modulates Akt activity to rewire metabolism and provide new survival/escape routes to breast cancer cells. We performed a mitochondrial stress test to monitor different parameters of mitochondrial respiration, including basal respiration, proton leak, maximal respiration, spare respiratory capacity, non-mitochondrial respiration, ATP production, and coupling efficiency. The 4-OHT+SEL combination did as well as or slightly better than the individual treatments in reducing different mitochondrial respiration parameters (Figure 4C). We also validated gene expression data related to metabolism using a glycolytic stress test, which monitors glycolysis, glycolytic capacity and glycolytic reserve. The 4-OHT+SEL combination was as good as or better than individual treatments in reducing all three parameters (Figure 4D). Next, we tested the individual and combinational effects of 4-OHT and SEL on the metabolic cell phenotypes of TAM-sensitive and TAM-resistant cell lines. Our results showed that although treatment with 4-OHT alone or SEL alone made all the cell lines less energetic, the cells became even more quiescent with the 4-OHT+SEL treatment (Figure 4E, Supplementary Figure S2). Of note, combining SEL with 4-OHT was as effective as combining a PI3K inhibitor (MK2206) with 4-OHT in reducing 4-OHT induced cell viability and increase in mitochondrial respiration (Supplementary Figure S3).

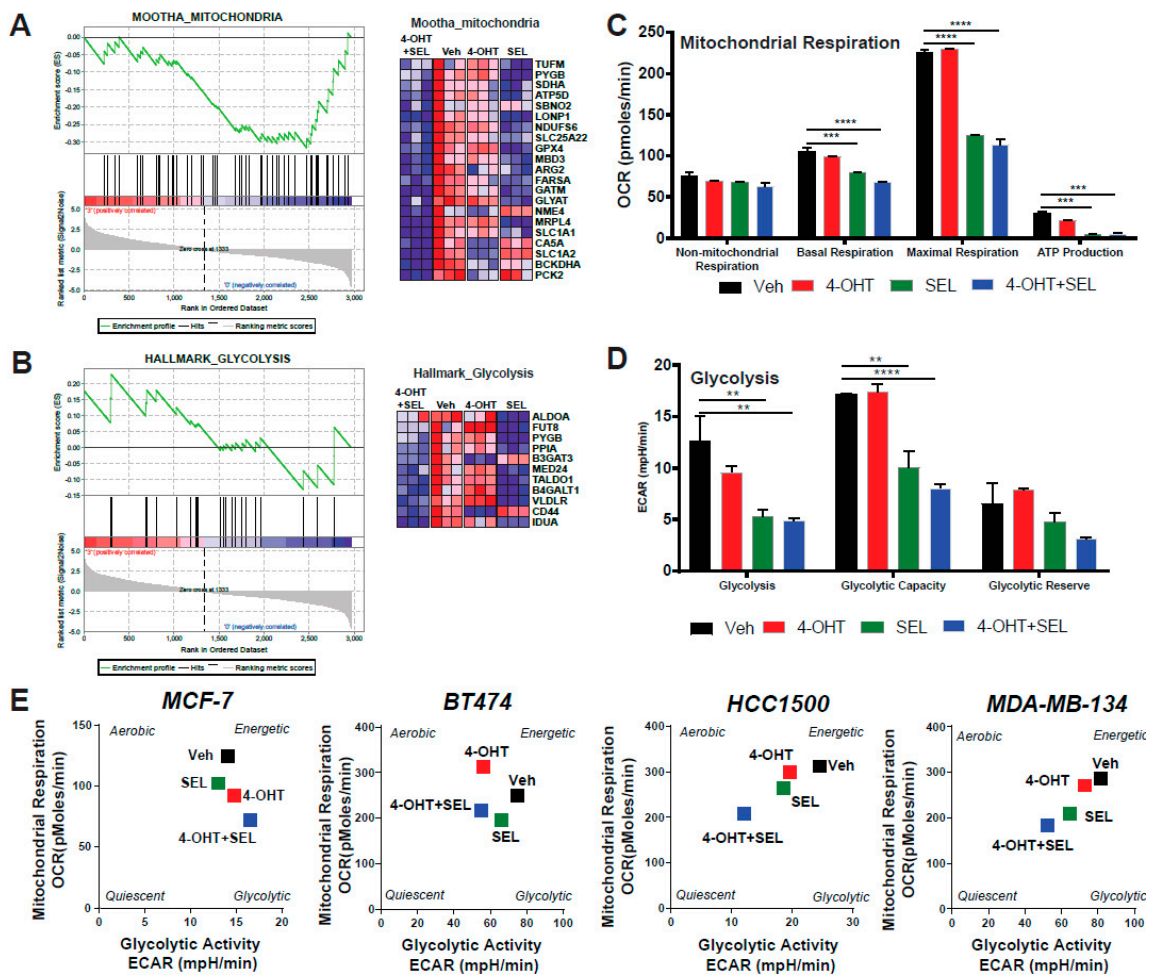


Figure 4. ER α -XPO1 targeting changes the metabolic phenotype of breast cancer cells from an energetic to a quiescent profile. GSEA analysis of RNA-Seq data depicting the regulation of glycolytic (A) and mitochondrial respiration (B) pathways by the 4-OHT+SEL combination. ER α -XPO1 targeting decreased the glycolytic activity of BT474 cells. Glycolytic functions were determined by the glycolysis stress test. A two-way analysis of variance (ANOVA) model was used for statistical significance of drug treatments alone or in combination and values were presented as mean \pm SEM from two independent experiments and all experiments were performed in triplicates. (* $p < 0.05$, ** $p < 0.01$, *** $p < 0.001$, **** $p < 0.0001$). (C,D) ER α -XPO1 targeting decreased the mitochondrial activity of BT474 cells. Mitochondrial activity parameters were measured by the mitochondrial stress test. A two-way analysis of variance (ANOVA) model was used for statistical significance calculations and values were presented as mean \pm SEM from three independent experiments (* $p < 0.05$, ** $p < 0.01$, *** $p < 0.001$, **** $p < 0.0001$). Some key parameters of mitochondrial function (Basal respiration, proton leak, maximal respiration, spare respiratory capacity, non-mitochondrial respiration, ATP production, coupling efficiency and spare respiratory capacity) were calculated and presented for each treatment conditions. (E) Cell phenotype assay resulted in MCF-7, BT474, MDA-MB-134 and HCC1500 cells, which were treated with 4-OHT (10–6 M) and SEL (10–7 M) for 24 h alone, for 24 h alone and in combination. Changes in metabolic profile was determined by measuring oxygen consumption rate (OCR) and extracellular acidification rate (ECAR) under basal and stressed conditions with the cell phenotype assay. Values are presented as \pm SEM from three independent experiments.

3.5. ER α -XPO1 Targeting Induces Autophagic Cell Death

Our gene expression analyses indicated that gene sets associated with cell cycle and regulation of epithelial cell proliferation were downregulated, whereas gene sets associated with autophagy and cell death were upregulated (Figure 5A). To validate these results, we performed cell cycle analysis in MCF-7

cells and BT474 cells treated with Veh, 4-OHT, SEL or the 4-OHT+SEL combination. The combination treatment was very effective, particularly in BT474 cells, in reducing ratio of S-phase cells (Figure 5B). We also validated autophagic vacuole formation (Figure 5C,D) and an increase in autophagy related proteins in this cell line (Figure 5E). In addition, we examined different apoptotic caspase activities, PARP cleavage and changes in apoptotic cells in both cell lines. We did not observe any indicator of apoptosis in either of the cell lines at up to 120 h of treatment (Supplementary Figure S3). Finally, treatment of BT474 cells with the autophagy inhibitor chloroquine blocked the 4-OHT+SEL mediated reduction in cell viability (Figure 5F). Together, these results reveal that co-inhibition of ER α -XPO1 leads to autophagic cell death.

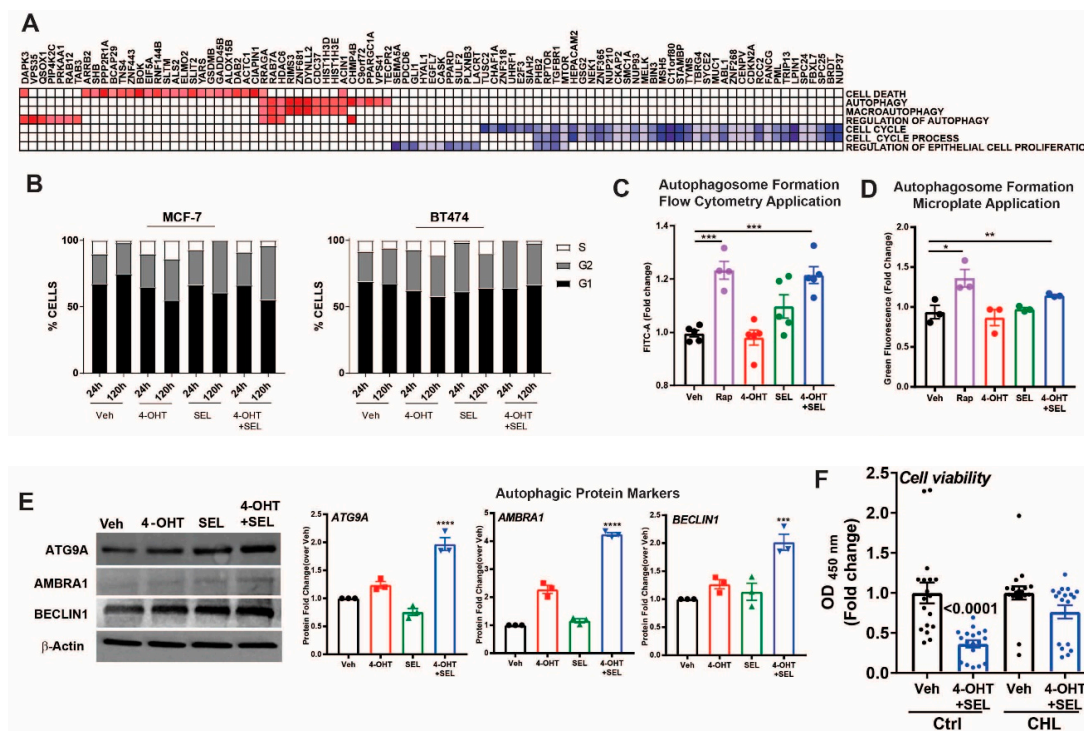


Figure 5. ER α -XPO1 targeting induces autophagic cell death. (A) GSEA analysis of cell proliferation and death pathways regulated by the 4-OHT+SEL combination treatment. (B) Cell cycle analysis after Veh, 4-OHT, SEL or 4-OHT+SEL treatments in MCF-7 and BT474 cells. LC3-II specific protein expression increased in TAM-resistant BT474 cells in a 24-h period. Comparison of the autophagic markers in BT474 cells treated with 4-OHT (10^{-6} M) and SEL (10^{-7} M) alone and in combination for 24 h. Autophagosome formation was detected with a colorimetric method (C) which measures the level of green fluorescent-labeled LC3-II specific signal or by FACS analysis of the cells after staining with antibodies specific for LC3-II (D). Rapamycin (50 nM) was used as a positive control for autophagy detection. A one-way analysis of variance (ANOVA) model was used for statistical significance of treatments. The experiment was performed in triplicates and values were presented as mean \pm SEM from two independent experiments (** $p < 0.01$, *** $p < 0.001$). (E) The western blot analysis showed that the level of autophagic protein markers are higher in BT474 cells treated with both 4-OHT (10^{-6} M) and SEL (10^{-7} M) compared to those treated with individual 4-OHT+SEL treatment. BT474 cells were seeded at a density of 1×10^5 cells/well and treated with 4-OHT (10^{-6} M) and SEL (10^{-7} M) alone and in combination. Protein expressions of autophagic proteins (ATG9A, AMBRA, ULK1 and Beclin-1) were detected with target specific antibodies at 1:1000 dilution. Protein signal was quantitated using Licor Odyssey. A one-way analysis of variance (ANOVA) model was used for statistical significance of treatment and values were presented as mean \pm SEM from three independent experimental repeats. (F) Autophagy inhibitor chloroquine inhibited 4OHT+SEL induced decrease in cell viability. One-way analysis of variance (ANOVA) model was used for statistical significance of treatments. (* $p < 0.05$, ** $p < 0.01$, *** $p < 0.001$).

4. Discussion

This study is the first of its kind to report the molecular basis of the effectiveness of the novel combination therapy of 4-OHT and SEL in providing sustained tumor regression for ER (+), Tam-resistant tumors. We showed that individual 4-OHT and SEL treatments increased differential Akt signaling in endocrine-resistant cells, but that the combination prevented this activation. We also reported transcriptional and functional consequences of combined ER α and XPO1 targeting. The combination therapy was the most efficient treatment at reversing the expression of endocrine resistance and metastasis-related gene expression programs. In addition, glycolytic and mitochondrial pathways were targeted by this combination. As a result, the 4-OHT+SEL combination effectively blocked glycolysis and mitochondrial respiration and caused cell death by activating autophagy. Our study is the first documented attempt to define the causal role of metabolic programming in therapy resistant ER (+) tumors and to explore the feasibility of the combined targeting of these pathways to improve the response to endocrine agents and decrease the risk of recurrence.

Targeting XPO1 together with ER α is clinically relevant for several reasons. First, in our published analysis from publicly available tumor datasets [11] and data from patient tumor samples (Figure 1A) mRNA and protein levels of XPO1 were higher in Luminal B subtype tumors, which are more likely to recur on endocrine treatments relative to Luminal A subtype. Second, high XPO1 mRNA expression was associated with a poor outcome in women who were treated with TAM [11]. And last, XPO1 was already being targeted in phase 2 and 3 clinical trials (clinicaltrials.gov) by SEL- a specific, covalent, small molecule orally bioavailable inhibitor of XPO1, to treat patients with hematological and solid cancers [22–24,42,43]. SEL is well tolerated with manageable side effects including nausea, fatigue and anorexia that improve over time on treatment. Even in patients that remained on therapy for more than 8 months, no significant cumulative drug toxicities have been identified [15]. Since cancer cells of different tumor types have been shown to be more sensitive to XPO1 inhibition than normal cells [44,45], combining TAM with SEL potentially offers higher efficacy, specificity and lower toxicity for treatment of endocrine resistant, recurrent ER (+) breast cancer.

We propose that co-targeting ER and XPO1 is an improved therapeutic strategy because inhibiting the proteins in combination caused both a metabolic shift and induced autophagy, which together led to prolonged tumor regression. The combined targeting of ER α and XPO1 overcame TAM resistance, modulated cellular signaling to prevent rewiring of tumor cell metabolism and induced cell death by autophagy (Figure 6). We showed that single or combined targeting of ER α and XPO1 caused differential regulation of Akt phosphorylation. The Akt pathway is a master regulator of cancer cell metabolism [46], components of PI3K/AKT/mTOR pathway are mutated in nearly 25% of breast tumors and are associated with drug responses in ER (+) and ER (–) tumors [47–49]. Estrogens stimulate this pathway to regulate migration and invasion of cancer cells characteristic of ER (+) tumors [50,51]. In return, mTOR signaling regulates the expression level and activity of ER α and mTOR acts as a coregulator for ER α [52,53]. Inhibition of PI3K increases ER expression and activity [48,54], and PI3K inhibitor-endocrine agent combinations were tested with minor success in clinical trials to treat women with endocrine resistant disease (NCT01339442, NCT02273973). Akt signaling regulates both aerobic glycolysis and oxidative phosphorylation and impact phenotypic features of tumor cells [55]. Our pathway activation assay showed that two established Akt targets, ENOS [56,57] and PLC γ -1 [58], which are associated with angiogenesis and metastasis [59], had increased phosphorylation levels when cells were treated with SEL only but not with the 4-OHT and SEL combination. A similar pattern of regulation was observed for p53 phosphorylation at Ser15 by SEL and Ser392 by 4-OHT. Interestingly, loss of Ser392 phosphorylation by p70S6K was shown to inhibit autophagy by decreasing expression of ULK1 in the context of oxidative stress [60] whereas the same modification by p38 MAPK activated autophagy [61]. Of note, p38 MAPK phosphorylation was increased only in the 4-OHT+SEL treated cells, which might explain why we observe autophagy only in this treatment condition.

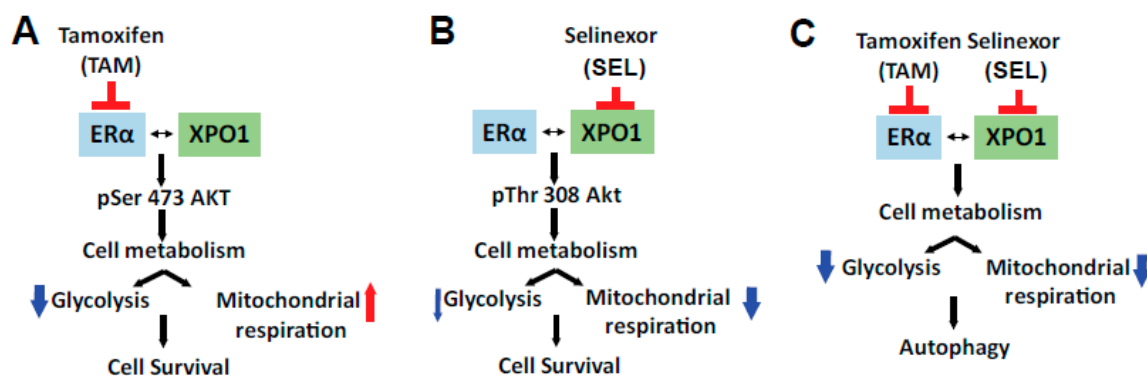


Figure 6. Molecular mechanism of sustained tumor regression by combined ER α -XPO1 targeting.

The majority of current research efforts in the therapy resistance field focuses on a delineation of the underlying mechanisms that lead to increased activity of selective signaling pathways. Undoubtedly, interrogating and targeting the end-point kinases in tumors are highly relevant and these studies lead to the development of combination therapies involving PI3K inhibitors or mTOR pathway inhibitors together with endocrine agents. However, resistance to these combination therapies also occurs, and in such cases, the cancer that develops is considerably more aggressive due to hyperactivation of compensatory mitogenic signaling pathways [62]. Moreover, these kinase inhibitors have many adverse side effects. More recently, ER α mutations that decrease sensitivity of the receptor to selective estrogen receptor modulators (SERMs) and selective estrogen receptor degraders (SERDs) were identified in about 15–40% of the metastatic, but not primary, tumors after AI treatment [63–67]. However, in ER (+) metastatic tumors that occur after TAM treatment, such mutations were not identified [68–70]. Our proposed treatment approach might prevent/delay the use of AIs and emergence of ESR1 mutations in tumors that recur after endocrine therapies, which is currently a significant clinical challenge.

Our studies described here provide a vast array of novel and important new information that will significantly advance our understanding of adaptive metabolic pathways associated with therapy resistance and cancer cell survival. The nuclear export pathways have not previously been implicated in TAM resistance and given the need for better strategies for selecting patients to receive TAM and improving therapeutic response of relapsed ER α (+) tumors, our results have great potential for uncovering the role of these pathways and their combined targeting in reducing recurrences and deaths due to metastatic ER (+) tumors. We expect our studies to establish a novel and innovative concept of combined targeting of ER α and XPO1 in TAM resistance that has not been previously explored in the field and will advance a new therapeutic strategy to the clinic. Successful translation of our findings to the clinic will change the treatment regimens for already metastasized patients while on TAM by replacing them with ones that are more effective, less toxic, and will positively impact the patient's survival.

5. Conclusions

In conclusion, ER α -XPO1 crosstalk is a driver of TAM-resistance by causing mislocalization of key factors. Co-targeting XPO1 and ER α in endocrine resistant tumors resensitizes tumors to TAM and achieve complete tumor regression by inhibiting cell metabolism and inducing autophagy. However, we do not know if we can combine XPO1 inhibitors with other therapies currently used in the clinics for treatment of metastatic BCAs and future preclinical studies are needed to answer these questions.

Supplementary Materials: The following are available online at <http://www.mdpi.com/2072-6694/11/4/479/s1>, Figure S1: Analysis of gene functional groups associated with different ligand treatments, Figure S2: Regulation of signaling pathways by 4-OHT and SEL, Figure S3: Combined ER α -XPO1 targeting cause apoptosis neither in MCF-7 nor in BT474 cells.

Author Contributions: Conceptualization, Z.M.-E.; methodology, E.K.-C., K.W., Y.C.Z., K.L.A.C., K.H., O.B.I., K.D., C.O., A.M., S.S. and H.C.; software, B.P.S.; validation, E.K.-C.; resources, S.S., B.H. and Y.L.; data curation,

E.K.-C., S.S., B.P.S. and Z.M.-E.; writing—original draft preparation, E.K.-C. and Z.M.-E.; writing—review and editing, E.K.-C., Y.L. and Z.M.-E., visualization, Z.M.-E. and B.P.S.; supervision, Z.M.-E.; project administration, Z.M.-E.; funding acquisition, Z.M.-E.

Funding: This work was supported by grants from the University of Illinois, Office of the Vice Chancellor for Research, Arnold O. Beckman award RB17083 (to Z.M.-E.), Karyopharm Investigator-initiated research grant (to Z.M.-E.) and National Institute of Food and Agriculture, U.S. Department of Agriculture, award ILLU-698-909 (to Z.M.-E.). C.O. and A.M. are part of the ResearchHStart, a program of the Cancer Center at Illinois at the Beckman Institute for Advanced Science and Technology, University of Illinois at Urbana-Champaign. The program is funded through philanthropic support from Ira and Debra Cohen, Kim Duchossois, and other generous donors.

Acknowledgments: We would like to thank Alvaro Hernandez and Chris Wright for help with RNA-Seq data generation.

Conflicts of Interest: Z.M.-E. is a coinventor on several patents entitled “Novel Compounds Which Activate Estrogen Receptors and Compositions and Methods of Using the Same”. Z.M.-E. was a PI on an investigator-initiated grant from Pfizer, Corteva Agrisciences and Karyopharm Therapeutics.

References

- Katzenellenbogen, B.S.; Frasar, J. Therapeutic targeting in the estrogen receptor hormonal pathway. *Semin. Oncol.* **2004**, *31*, 28–38. [[CrossRef](#)] [[PubMed](#)]
- Rugo, H.S.; Rumble, R.B.; Macrae, E.; Barton, D.L.; Connolly, H.K.; Dickler, M.N.; Fallowfield, L.; Fowble, B.; Ingle, J.N.; Jahanzeb, M.; et al. Endocrine Therapy for Hormone Receptor-Positive Metastatic Breast Cancer: American Society of Clinical Oncology Guideline. *J. Clin. Oncol.* **2016**, *34*, 3069–3103. [[CrossRef](#)]
- Yu, K.-D.; Wu, J.; Shen, Z.-Z.; Shao, Z.-M. Hazard of Breast Cancer-Specific Mortality among Women with Estrogen Receptor-Positive Breast Cancer after Five Years from Diagnosis: Implication for Extended Endocrine Therapy. *J. Clin. Endocrinol. Metab.* **2012**, *97*, E2201–E2209. [[CrossRef](#)] [[PubMed](#)]
- Jatoi, I.; Anderson, W.F.; Jeong, J.-H.; Redmond, C.K. Breast Cancer Adjuvant Therapy: Time to Consider Its Time-Dependent Effects. *J. Clin. Oncol.* **2011**, *29*, 2301–2304. [[CrossRef](#)] [[PubMed](#)]
- Burstein, H.J.; Temin, S.; Anderson, H.; Buchholz, T.A.; Davidson, N.E.; Gelmon, K.E.; Giordano, S.H.; Hudis, C.A.; Rowden, D.; Solky, A.J.; et al. Adjuvant Endocrine Therapy for Women with Hormone Receptor-Positive Breast Cancer: American Society of Clinical Oncology Clinical Practice Guideline Focused Update. *J. Clin. Oncol.* **2014**, *32*, 2255–2269. [[CrossRef](#)]
- Colleoni, M.; Sun, Z.; Price, K.N.; Karlsson, P.; Forbes, J.F.; Thurlimann, B.; Gianni, L.; Castiglione, M.; Gelber, R.D.; Coates, A.S.; et al. Annual Hazard Rates of Recurrence for Breast Cancer During 24 Years of Follow-Up: Results from the International Breast Cancer Study Group Trials I to V. *J. Clin. Oncol.* **2016**, *34*, 927–935. [[CrossRef](#)] [[PubMed](#)]
- Pan, H.; Gray, R.; Braybrooke, J.; Davies, C.; Taylor, C.; McGale, P.; Peto, R.; Pritchard, K.I.; Bergh, J.; Dowsett, M.; et al. 20-Year Risks of Breast-Cancer Recurrence after Stopping Endocrine Therapy at 5 Years. *N. Engl. J. Med.* **2017**, *377*, 1836–1846. [[CrossRef](#)]
- Jatoi, I.; Chen, B.E.; Anderson, W.F.; Rosenberg, P.S. Breast cancer mortality trends in the United States according to estrogen receptor status and age at diagnosis. *J. Clin. Oncol.* **2007**, *25*, 1683–1690. [[CrossRef](#)]
- Kulkoyluoglu, E.; Madak-Erdogan, Z. Nuclear and extranuclear-initiated estrogen receptor signaling crosstalk and endocrine resistance in breast cancer. *Steroids* **2016**, *114*, 41–47. [[CrossRef](#)]
- Howell, A.; Cuzick, J.; Baum, M.; Buzdar, A.; Dowsett, M.; Forbes, J.F.; Hoctin-Boes, G.; Houghton, J.; Locker, G.Y.; Tobias, J.S. Results of the ATAC (Arimidex, Tamoxifen, Alone or in Combination) trial after completion of 5 years' adjuvant treatment for breast cancer. *Lancet* **2005**, *365*, 60–62.
- Wrobel, K.; Zhao, Y.C.; Kulkoyluoglu, E.; Chen, K.L.; Hieronymi, K.; Holloway, J.; Li, S.; Ray, T.; Ray, P.S.; Landesman, Y.; et al. ER α -XPO1 Cross Talk Controls Tamoxifen Sensitivity in Tumors by Altering ERK5 Cellular Localization. *Mol. Endocrinol.* **2016**, *30*, 1029–1045. [[CrossRef](#)]
- Turner, J.G.; Dawson, J.L.; Grant, S.; Shain, K.H.; Dalton, W.S.; Dai, Y.; Meads, M.; Baz, R.; Kauffman, M.; Shacham, S.; et al. Treatment of acquired drug resistance in multiple myeloma by combination therapy with XPO1 and topoisomerase II inhibitors. *J. Hematol. Oncol.* **2016**, *9*, 73. [[CrossRef](#)]

13. Gravina, G.L.; Tortoreto, M.; Mancini, A.; Addis, A.; Di Cesare, E.; Lenzi, A.; Landesman, Y.; McCauley, D.; Kauffman, M.; Shacham, S.; et al. XPO1/CRM1-selective inhibitors of nuclear export (SINE) reduce tumor spreading and improve overall survival in preclinical models of prostate cancer (PCa). *J. Hematol. Oncol.* **2014**, *7*, 46. [[CrossRef](#)]
14. Neggers, J.E.; Vercruyse, T.; Jacquemyn, M.; Vanstreels, E.; Baloglu, E.; Shacham, S.; Crochiere, M.; Landesman, Y.; Daelemans, D. Identifying drug-target selectivity of small-molecule CRM1/XPO1 inhibitors by CRISPR/Cas9 genome editing. *Chem. Biol.* **2015**, *22*, 107–116. [[CrossRef](#)]
15. Chen, C.I.; Gutierrez, M.; Brown, P.N.; Gabrail, N.; Baz, R.; Reece, D.E.; Savona, M.; Trudel, S.; Siegel, D.S.; Mau-Sorensen, M.; et al. Anti Tumor Activity Of Selinexor (KPT-330), A First-In-Class Oral Selective Inhibitor Of Nuclear Export (SINE) XPO1/CRM1 Antagonist In Patients (pts) With Relapsed/Refractory Multiple Myeloma (MM) Or Waldenstrom’s Macroglobulinemia (WM). *Blood* **2013**, *122*, 1942.
16. Bergamaschi, A.; Madak-Erdogan, Z.; Kim, Y.J.; Choi, Y.L.; Lu, H.; Katzenellenbogen, B.S. The forkhead transcription factor FOXM1 promotes endocrine resistance and invasiveness in estrogen receptor-positive breast cancer by expansion of stem-like cancer cells. *Breast Cancer Res.* **2014**, *16*, 436. [[CrossRef](#)]
17. Holliday, D.L.; Speirs, V. Choosing the right cell line for breast cancer research. *Breast Cancer Res.* **2011**, *13*, 215. [[CrossRef](#)]
18. Zhang, X.; Mu, X.; Huang, O.; Xie, Z.; Jiang, M.; Geng, M.; Shen, K. Luminal breast cancer cell lines overexpressing ZNF703 are resistant to tamoxifen through activation of Akt/mTOR signaling. *PLoS ONE* **2013**, *8*, e72053. [[CrossRef](#)]
19. Chen, K.L.A.; Zhao, Y.C.; Hieronymi, K.; Smith, B.P.; Madak-Erdogan, Z. Bazedoxifene and conjugated estrogen combination maintains metabolic homeostasis and benefits liver health. *PLoS ONE* **2017**, *12*, e0189911. [[CrossRef](#)]
20. Madak-Erdogan, Z.; Kim, S.H.; Gong, P.; Zhao, Y.C.; Zhang, H.; Chambliss, K.L.; Carlson, K.E.; Mayne, C.G.; Shaul, P.W.; Korach, K.S.; et al. Design of pathway preferential estrogens that provide beneficial metabolic and vascular effects without stimulating reproductive tissues. *Sci. Signal.* **2016**, *9*, ra53. [[CrossRef](#)]
21. Zhao, Y.C.; Madak Erdogan, Z. Systems Biology of Metabolic Regulation by Estrogen Receptor Signaling in Breast Cancer. *J. Vis. Exp.* **2016**. [[CrossRef](#)]
22. Alexander, T.B.; Lacayo, N.J.; Choi, J.K.; Ribeiro, R.C.; Pui, C.-H.; Rubnitz, J.E. Phase I Study of Selinexor, a Selective Inhibitor of Nuclear Export, in Combination with Fludarabine and Cytarabine, in Pediatric Relapsed or Refractory Acute Leukemia. *J. Clin. Oncol.* **2016**, *34*, 4094–4101. [[CrossRef](#)]
23. Gounder, M.M.; Zer, A.; Tap, W.D.; Salah, S.; Dickson, M.A.; Gupta, A.A.; Keohan, M.L.; Loong, H.H.; D’Angelo, S.P.; Baker, S.; et al. Phase IB Study of Selinexor, a First-in-Class Inhibitor of Nuclear Export, in Patients With Advanced Refractory Bone or Soft Tissue Sarcoma. *J. Clin. Oncol.* **2016**, *34*, 3166–3174. [[CrossRef](#)]
24. Razak, A.R.A.; Mau-Soerensen, M.; Gabrail, N.Y.; Gerecitano, J.F.; Shields, A.F.; Unger, T.J.; Saint-Martin, J.R.; Carlson, R.; Landesman, Y.; McCauley, D.; et al. First-in-Class, First-in-Human Phase I Study of Selinexor, a Selective Inhibitor of Nuclear Export, in Patients with Advanced Solid Tumors. *J. Clin. Oncol.* **2016**, *34*, 4142–4150. [[CrossRef](#)]
25. Bolger, A.M.; Lohse, M.; Usadel, B. Trimmomatic: A flexible trimmer for Illumina sequence data. *Bioinformatics* **2014**, *30*, 2114–2120. [[CrossRef](#)]
26. Zerbino, D.R.; Achuthan, P.; Akanni, W.; Amode, M.R.; Barrell, D.; Bhai, J.; Billis, K.; Cummins, C.; Gall, A.; Girón, C.G.; et al. Ensembl 2018. *Nucleic Acids Res.* **2018**, *46*, D754–D761. [[CrossRef](#)]
27. Dobin, A.; Davis, C.A.; Schlesinger, F.; Drenkow, J.; Zaleski, C.; Jha, S.; Batut, P.; Chaisson, M.; Gingeras, T.R. STAR: ultrafast universal RNA-seq aligner. *Bioinformatics* **2013**, *29*, 15–21. [[CrossRef](#)]
28. Liao, Y.; Smyth, G.K.; Shi, W. The Subread aligner: Fast, accurate and scalable read mapping by seed-and-vote. *Nucleic Acids Res.* **2013**, *41*, e108. [[CrossRef](#)]
29. Robinson, M.D.; McCarthy, D.J.; Smyth, G.K. edgeR: A Bioconductor package for differential expression analysis of digital gene expression data. *Bioinformatics* **2010**, *26*, 139–140. [[CrossRef](#)]
30. Ritchie, M.E.; Phipson, B.; Wu, D.; Hu, Y.; Law, C.W.; Shi, W.; Smyth, G.K. Limma powers differential expression analyses for RNA-sequencing and microarray studies. *Nucleic Acids Res.* **2015**, *43*, e47. [[CrossRef](#)]
31. Phipson, B.; Lee, S.; Majewski, I.J.; Alexander, W.S.; Smyth, G.K. Robust hyperparameter estimation protects against hypervariable genes and improves power to detect differential expression. *Ann. Appl. Stat.* **2016**, *10*, 946–963. [[CrossRef](#)]

32. Benjamini, Y.; Hochberg, Y. Controlling the False Discovery Rate: A Practical and Powerful Approach to Multiple Testing. *J. R. Stat. Soc. Ser. B (Methodol.)* **1995**, *57*, 289–300. [[CrossRef](#)]
33. Subramanian, A.; Tamayo, P.; Mootha, V.K.; Mukherjee, S.; Ebert, B.L.; Gillette, M.A.; Paulovich, A.; Pomeroy, S.L.; Golub, T.R.; Lander, E.S.; et al. Gene set enrichment analysis: A knowledge-based approach for interpreting genome-wide expression profiles. *Proc. Natl. Acad. Sci. USA* **2005**, *102*, 15545–15550. [[CrossRef](#)]
34. Mootha, V.K.; Lindgren, C.M.; Eriksson, K.-F.; Subramanian, A.; Sihag, S.; Lehar, J.; Puigserver, P.; Carlsson, E.; Ridderstråle, M.; Laurila, E.; et al. PGC-1 α -responsive genes involved in oxidative phosphorylation are coordinately downregulated in human diabetes. *Nat. Genet.* **2003**, *34*, 267. [[CrossRef](#)]
35. Arpino, G.; Gutierrez, C.; Weiss, H.; Rimawi, M.; Massarweh, S.; Bharwani, L.; De Placido, S.; Osborne, C.K.; Schiff, R. Treatment of human epidermal growth factor receptor 2-overexpressing breast cancer xenografts with multiagent HER-targeted therapy. *J. Natl. Cancer Inst.* **2007**, *99*, 694–705. [[CrossRef](#)]
36. Wang, C.X.; Koay, D.C.; Edwards, A.; Lu, Z.; Mor, G.; Ocal, I.T.; Digiovanna, M.P. In vitro and in vivo effects of combination of Trastuzumab (Herceptin) and Tamoxifen in breast cancer. *Breast Cancer Res. Treat.* **2005**, *92*, 251–263. [[CrossRef](#)]
37. Kondov, B.; Milenković, Z.; Kondov, G.; Petrushevska, G.; Basheska, N.; Bogdanovska-Todorovska, M.; Tolevska, N.; Ivković, L. Presentation of the Molecular Subtypes of Breast Cancer Detected By Immunohistochemistry in Surgically Treated Patients. *Open Access Maced. J. Med. Sci.* **2018**, *6*, 961–967. [[CrossRef](#)]
38. Inic, Z.; Zegarac, M.; Inic, M.; Markovic, I.; Kozomara, Z.; Djuricic, I.; Inic, I.; Pupic, G.; Jancic, S. Difference between Luminal A and Luminal B Subtypes According to Ki-67, Tumor Size, and Progesterone Receptor Negativity Providing Prognostic Information. *Clinical Medicine Insights. Oncology* **2014**, *8*, 107–111. [[CrossRef](#)]
39. Madak-Erdogan, Z.; Charn, T.H.; Jiang, Y.; Liu, E.T.; Katzenellenbogen, J.A.; Katzenellenbogen, B.S. Integrative genomics of gene and metabolic regulation by estrogen receptors alpha and beta, and their coregulators. *Mol. Syst. Biol.* **2013**, *9*, 676. [[CrossRef](#)]
40. Giltane, J.M.; Hutchinson, K.E.; Stricker, T.P.; Formisano, L.; Young, C.D.; Estrada, M.V.; Nixon, M.J.; Du, L.; Sanchez, V.; Ericsson, P.G.; et al. Genomic profiling of ER+ breast cancers after short-term estrogen suppression reveals alterations associated with endocrine resistance. *Sci. Transl. Med.* **2017**, *9*, eaai7993. [[CrossRef](#)]
41. Formisano, L.; Lu, Y.; Jansen, V.M.; Bauer, J.A.; Hanker, A.B.; Sanders, M.E.; González-Ericsson, P.; Kim, S.; Arnedos, M.; André, F.; et al. Abstract 1008: Gain-of-function kinase library screen identifies FGFR1 amplification as a mechanism of resistance to antiestrogens and CDK4/6 inhibitors in ER+ breast cancer. *Cancer Res.* **2017**, *77*, 1008. [[CrossRef](#)]
42. Ranganathan, P.; Kashyap, T.; Yu, X.; Meng, X.; Lai, T.-H.; McNeil, B.; Bhatnagar, B.; Shacham, S.; Kauffman, M.; Dorrance, A.M.; et al. XPO1 Inhibition using Selinexor Synergizes with Chemotherapy in Acute Myeloid Leukemia by Targeting DNA Repair and Restoring Topoisomerase II α to the Nucleus. *Clin. Cancer Res.* **2016**, *22*, 6142–6152. [[CrossRef](#)]
43. Kuruvilla, J.; Savona, M.; Baz, R.; Mau-Sorensen, P.M.; Gabrail, N.; Garzon, R.; Stone, R.; Wang, M.; Savoie, L.; Martin, P.; et al. Selective inhibition of nuclear export with selinexor in patients with non-Hodgkin lymphoma. *Blood* **2017**, *129*, 3175–3183. [[CrossRef](#)]
44. Salas Fragomeni, R.A.; Chung, H.W.; Landesman, Y.; Senapedis, W.; Saint-Martin, J.R.; Tsao, H.; Flaherty, K.T.; Shacham, S.; Kauffman, M.; Cusack, J.C. CRM1 and BRAF inhibition synergize and induce tumor regression in BRAF-mutant melanoma. *Mol. Cancer Ther.* **2013**, *12*, 1171–1179. [[CrossRef](#)]
45. Turner, J.G.; Marchion, D.C.; Dawson, J.L.; Emmons, M.F.; Hazlehurst, L.A.; Washausen, P.; Sullivan, D.M. Human multiple myeloma cells are sensitized to topoisomerase II inhibitors by CRM1 inhibition. *Cancer Res.* **2009**, *69*, 6899–6905. [[CrossRef](#)]
46. Hanahan, D.; Robert Weinberg, A. Hallmarks of Cancer: The Next Generation. *Cell* **2011**, *144*, 646–674. [[CrossRef](#)]
47. Yndestad, S.; Austreid, E.; Svanberg, I.R.; Knappskog, S.; Lønning, P.E.; Eikesdal, H.P. Activation of Akt characterizes estrogen receptor positive human breast cancers which respond to anthracyclines. *Oncotarget* **2017**, *8*, 41227–41241. [[CrossRef](#)]

48. Bosch, A.; Li, Z.; Bergamaschi, A.; Ellis, H.; Toska, E.; Prat, A.; Tao, J.J.; Spratt, D.E.; Viola-Villegas, N.T.; Castel, P.; et al. PI3K inhibition results in enhanced estrogen receptor function and dependence in hormone receptor-positive breast cancer. *Sci. Transl. Med.* **2015**, *7*, 283ra51. [[CrossRef](#)]
49. Bostner, J.; Karlsson, E.; Pandiyan, M.J.; Westman, H.; Skoog, L.; Fornander, T.; Nordenskjöld, B.; Stål, O. Activation of Akt, mTOR, and the estrogen receptor as a signature to predict tamoxifen treatment benefit. *Breast Cancer Res. Treat.* **2013**, *137*, 397–406. [[CrossRef](#)]
50. Zhou, K.; Sun, P.; Zhang, Y.; You, X.; Li, P.; Wang, T. Estrogen stimulated migration and invasion of estrogen receptor-negative breast cancer cells involves an ezrin-dependent crosstalk between G protein-coupled receptor 30 and estrogen receptor beta signaling. *Steroids* **2016**, *111*, 113–120. [[CrossRef](#)]
51. Zhang, G. Upregulation of estrogen receptor mediates migration, invasion and proliferation of endometrial carcinoma cells by regulating the PI3K/AKT/mTOR pathway. *Oncol. Rep.* **2014**, *31*, 1175–1182.
52. Alayev, A.; Salamon, R.S.; Berger, S.M.; Schwartz, N.S.; Cuesta, R.; Snyder, R.B.; Holz, M.K. mTORC1 directly phosphorylates and activates ERalpha upon estrogen stimulation. *Oncogene* **2016**, *35*, 3535–3543. [[CrossRef](#)]
53. Shrivastav, A.; Bruce, M.; Jaksic, D.; Bader, T.; Seekallu, S.; Penner, C.; Nugent, Z.; Watson, P.; Murphy, L. The mechanistic target for rapamycin pathway is related to the phosphorylation score for estrogen receptor-alpha in human breast tumors in vivo. *Breast Cancer Res.* **2014**, *16*, R49. [[CrossRef](#)]
54. Toska, E.; Osmanbeyoglu, H.U.; Castel, P.; Chan, C.; Hendrickson, R.C.; Elkabets, M.; Dickler, M.N.; Scaltriti, M.; Leslie, C.S.; Armstrong, S.A.; et al. PI3K pathway regulates ER-dependent transcription in breast cancer through the epigenetic regulator KMT2D. *Science* **2017**, *355*, 1324–1330. [[CrossRef](#)]
55. Robey, R.B.; Hay, N. Is Akt the “Warburg kinase”?—Akt-energy metabolism interactions and oncogenesis. *Semin. Cancer Biol.* **2009**, *19*, 25–31. [[CrossRef](#)]
56. Michell, B.J.; Griffiths, J.E.; Mitchelhill, K.I.; Rodriguez-Crespo, I.; Tiganis, T.; Bozinovski, S.; de Montellano, P.R.O.; Kemp, B.E.; Pearson, R.B. The Akt kinase signals directly to endothelial nitric oxide synthase. *Curr. Biol.* **1999**, *9*, 845–848. [[CrossRef](#)]
57. Fulton, D.; Gratton, J.-P.; McCabe, T.J.; Fontana, J.; Fujio, Y.; Walsh, K.; Franke, T.F.; Papapetropoulos, A.; Sessa, W.C. Regulation of endothelium-derived nitric oxide production by the protein kinase Akt. *Nature* **1999**, *399*, 597–601. [[CrossRef](#)]
58. Wang, Y.; Wu, J.; Wang, Z. Akt Binds to and Phosphorylates Phospholipase C-γ1 in Response to Epidermal Growth Factor. *Mol. Biol. Cell* **2006**, *17*, 2267–2277. [[CrossRef](#)]
59. Balz, L.M.; Bartkowiak, K.; Andreas, A.; Pantel, K.; Niggemann, B.; Zänker, K.S.; Brandt, B.H.; Dittmar, T. The interplay of HER2/HER3/PI3K and EGFR/HER2/PLC-γ1 signalling in breast cancer cell migration and dissemination. *J. Pathol.* **2012**, *227*, 234–244. [[CrossRef](#)]
60. Ci, Y.; Shi, K.; An, J.; Yang, Y.; Hui, K.; Wu, P.; Shi, L.; Xu, C. ROS inhibit autophagy by downregulating ULK1 mediated by the phosphorylation of p53 in selenite-treated NB4 cells. *Cell Death Dis.* **2014**, *5*, e1542. [[CrossRef](#)]
61. Liu, B.; Cheng, Y.; Zhang, B.; Bian, H.-J.; Bao, J.-K. Polygonatum cyrtoneuma lectin induces apoptosis and autophagy in human melanoma A375 cells through a mitochondria-mediated ROS–p38–p53 pathway. *Cancer Lett.* **2009**, *275*, 54–60. [[CrossRef](#)]
62. Dees, E.C.; Carey, L.A. Improving endocrine therapy for breast cancer: It’s not that simple. *J. Clin. Oncol.* **2013**, *31*, 171–173. [[CrossRef](#)]
63. Alluri, P.G.; Speers, C.; Chinnaiyan, A.M. Estrogen receptor mutations and their role in breast cancer progression. *Breast Cancer Res.* **2014**, *16*, 494. [[CrossRef](#)]
64. Chu, D.; Paoletti, C.; Gersch, C.; Van Den Berg, D.; Zabransky, D.; Cochran, R.; Wong, H.Y.; Valda Toro, P.; Cidado, J.; Croessmann, S.; et al. ESR1 mutations in circulating plasma tumor DNA from metastatic breast cancer patients. *Clin. Cancer Res.* **2016**, *22*, 993–999. [[CrossRef](#)]
65. Li, S.; Shen, D.; Shao, J.; Crowder, R.; Liu, W.; Prat, A.; He, X.; Liu, S.; Hoog, J.; Lu, C.; et al. Endocrine-therapy-resistant ESR1 variants revealed by genomic characterization of breast-cancer-derived xenografts. *Cell Rep.* **2013**, *4*, 1116–1130. [[CrossRef](#)]
66. Robinson, D.R.; Wu, Y.M.; Vats, P.; Su, F.; Lonigro, R.J.; Cao, X.; Kalyana-Sundaram, S.; Wang, R.; Ning, Y.; Hodges, L.; et al. Activating ESR1 mutations in hormone-resistant metastatic breast cancer. *Nat. Genet.* **2013**, *45*, 1446–1451. [[CrossRef](#)]

67. Toy, W.; Shen, Y.; Won, H.; Green, B.; Sakr, R.A.; Will, M.; Li, Z.; Gala, K.; Fanning, S.; King, T.A.; et al. ESR1 ligand-binding domain mutations in hormone-resistant breast cancer. *Nat. Genet.* **2013**, *45*, 1439–1445. [[CrossRef](#)]
68. Jeselsohn, R.; Yelensky, R.; Buchwalter, G.; Frampton, G.; Meric-Bernstam, F.; Gonzalez-Angulo, A.M.; Ferrer-Lozano, J.; Perez-Fidalgo, J.A.; Cristofanilli, M.; Gómez, H.; et al. Emergence of Constitutively Active Estrogen Receptor- α Mutations in Pretreated Advanced Estrogen Receptor-Positive Breast Cancer. *Clin. Cancer Res.* **2014**, *20*, 1757–1767. [[CrossRef](#)]
69. Fribbens, C.; O’Leary, B.; Kilburn, L.; Hrebien, S.; Garcia-Murillas, I.; Beaney, M.; Cristofanilli, M.; Andre, F.; Loi, S.; Loibl, S.; et al. Plasma ESR1 Mutations and the Treatment of Estrogen Receptor-Positive Advanced Breast Cancer. *J. Clin. Oncol.* **2016**, *34*, 2961–2968. [[CrossRef](#)]
70. Schiavon, G.; Hrebien, S.; Garcia-Murillas, I.; Cutts, R.J.; Pearson, A.; Tarazona, N.; Fenwick, K.; Kozarewa, I.; Lopez-Knowles, E.; Ribas, R.; et al. Analysis of *ESR1* mutation in circulating tumor DNA demonstrates evolution during therapy for metastatic breast cancer. *Sci. Transl. Med.* **2015**, *7*, ra182–ra313. [[CrossRef](#)]



© 2019 by the authors. Licensee MDPI, Basel, Switzerland. This article is an open access article distributed under the terms and conditions of the Creative Commons Attribution (CC BY) license (<http://creativecommons.org/licenses/by/4.0/>).